LoGait: LoRa Sensing System of Human Gait Recognition using Dynamic Time Wraping

Yao Ge[1], Wenda Li[2], Muhammad Farooq[1], Adnan Qayyum[1], Jingyan Wang[1], Zikang Chen[1], Jonathan Cooper[1]
Muhammad Ali Imran[1], and Qammer H. Abbasi[1]

[1]James Watt School of Engineering, University of Glasgow, UK
[2]Department of Biomedical Engineering, University of Dundee, UK

***Abstract*—Vision-based gait analysis and human identification systems have been widely proposed in the literature. However, these systems cannot be readily applied in many real-time applications due to involved challenges such as video quality, occlusion, and serious privacy concerns. To overcome such issues, we propose the LoGait system that leverages ubiqutous LoRa signals recognise gait in different indoor environments. Our work is based on the intuition that the walking pattern of different users can be distinguished by distinct stride size and frequency. The wireless LoRa signal which is interfered by human walking will capture the gait information of subjects. In combination with the long-distance transmission ability of LoRa signal, the system enables a larger sensing range of gait recognition compared to the WiFi-based gait recognition system. The proposed LoGait system utilizes the phase difference between two LoRa receive channels, along with a set of filtering techniques, to extract distinctive features and generate a human gait profile. This profile is then matched against a database using a dynamic time wraping (DTW) based recognition algorithm, enabling accurate identification based on unique gait patterns. It has been validated in three different scenarios for gait recognition namely line of sight (LOS), non-line of sight (NLOS), and long-distance, with accuracy of 85.13%, 79.14%, and 84.14%, respectively.**

***Index Terms*—LoRa sensing, gait recognition, machine learning, dynamic time wrapping**

I. Introduction

In recent years, joint sensing and communication (JSAC) using wireless signals have been widely studied for different future smart home systems and other sensing applications [1]–[4]. Sensing with such RF signals is not in itself a new concept in research. The phenomena depend upon the analysis using the radio signal transmission and reception parameters, using the same principles developed to detect the presence of objects in aircraft radar and sonar systems. In wireless transmission systems, the transmission signal's attenuation is inevitable due to path loss, shadowing, and multi-path fading [5]. On the other hand, these attenuations on the wireless channel can be used to map the physical environment where the RF signals are propagating, providing the theoretical underpinning principle for contactless sensing. Using a communication wireless signal is the most cost-efficient way to perform RF sensing since it is easily accessible in most indoor spaces.

The growing interest in JSAC-based sensing systems is due to their practical deployments in indoor settings, as well as their ability to gain responses from monitored persons. Using ambient wireless signals like LoRa and WiFi rather than a camera provides three advantages. First, it preserves the users' privacy—without requiring them to record videos of daily life activities. Secondly, it resolves the limitations of video-based analysis by allowing sensing through-wall and dark spaces. Last but not the least, the utilisation of ambient signals like LoRa and WiFi reduces the cost. Although it requires computation resources to support the sensing algorithm like edge computing, the system's transceiver units are provided by current communication facilities.

A. Related Works

This section gives a overview of previous researches in JSAC and gait recognition respectively with the listed works shown in Table. I. Gait recognition is one of the human recognition methods as gait provide features that are highly related to specific person [6]. The gait recognition method nowadays is vision based mostly. However, recording video or picture can cause privacy issues. In addition, vision based gait recognition is limited with the working scenery. To address these problems, gait recognition based on different sensors is proposed [7].

JSAC is a concept that involves combining sensing and communication functions in a single device or system. This approach can lead to increased efficiency of communication and cost savings, as well as improved performance of sensing. This concept is becoming increasingly important as the Internet of Things (IoT) and other connected devices continue to grow in popularity. Recently, the main sensing techniques in this area are about WiFi, Radio Frequency Identification (RFID) and Ultra-Wide-bandwidth (UWB). Typically, WiFi is one of popular topic in this field due to the high cost-effectiveness compared to other sensors. In [8], [9], two WiFi based human activity recognition system are proposed. Both systems achieved over 95% accuracy in recognizing human activities. WiFi is also used in gait recognition [10], [11], the WiDIGR proposed in [10] achieved 78.28% accuracy in 6 subjects gait recognition. UWB based systems are also commonly used in different situation, including gesture recognition [17], gait recognition [12], [13] and human activity recognition [14]. In [15], RFID is also used in recognizing the fluid taking gesture. However, all mentioned systems mentioned above are limited with the sensing distance. LoRa based systems have only a few works in sensing topic but has shown its availability

TABLE I: Review of RF sensing works

Reference	Protocol	Carrier Frequency	Bandwidth	Application	Experimental Setup Range / Subjects	Performance
CARM [8]	WiFi	5 GHz	20 MHz* 30 subcarriers	human activity recognition	7.7*6.5M/ 25 subjects	8 activities recognition with over 96.5% accuracy in average
HARNN [9]	WiFi	5 GHz	20 MHz* 30 subcarriers	human activity recognition	indoor 5*6m, 8*6m/10 subjects	6 activities recognition with over 95% accuracy in average.
WiDIGR [10]	WiFi	5.825 GHz	20MHz* 30 subcarriers	gait recognition	5*5m / 60 subjects	78.28% accuracy for 6 subjects recognition
CAUTION [11]	WiFi	5 GHz	40MHz* 114 subcarriers	gait recognition	5.8*6.3 m 7.2*5.2 m/ 20 subjects	88% accuracy in 15 subjects identification
[12]	UWB	4.3 GHz	2 GHz	gait recognition	3m in chamber / Not mentioned	normal and spastic gait recognition with 94.9% accuracy
[13]	FMCW and UWB radar	25 GHz FMCW/ 7.5 GHz UWB	2GHz FMCW/ 1.5GHz UWB	gait recognition	2.7*1.8m / 14 subjects	Gait recognition in 14 subjects with 84% accuracy in average
[14]	UWB	5.2 GHz	8.7 GHz	human activity recognition	2.5m / 13 subjects	12 non-in-situ motions recognition with an average of 88.9% accuracy, in-situ motions 89.7% average accuracy.
[15]	UHF RFID	865 MHz	3 MHz	gestures recognition	2.5m / 15 subjects	87% accuracy for recognition of drinking episodes for young volunteers and 79% for older volunteers
[16]	LoRa	915 MHz	**125 kHz**	respiration sensing/ human tracking	**25m(respiration)/ 35m(tracking)**	Achieve long-range through-wall respiration sensing with 0.25bpm mean absolute error, human tracking with 4.27cm average absolute error.
LoGait (Ours)	LoRa	868.1 MHz	**125 kHz**	gait recognition	**5m, 20m (LOS)** & **6m(NLOS)** /13 subjects	Adopt LoRa signals to extend the gait recognition in various environment including 20m corridor, with 82.8% accuracy.

in long-range detection [16], [18]. As Table. I shows, the maximum sensing range of WiFi, UWB and RFID system is limited in 8m, 3m and 2.5m respectively. In comparison, LoRa system proposed in [16] extend the sensing range to 35m for human tracking and 25m for respiration monitor. Another work presents the similar result but tested through-wall respiration detection [18]. And our proposed LoGait system also push the gait recognition to the range of $20m$ compared to the previous WiFi scheme of WiDIGR [10] of $5m$ and CAUTION [11] of $7m$. Furthermore, the LoRa signal utilized in our system demonstrates enhanced penetration capabilities through obstacles, making it particularly suitable for indoor through-wall sensing, which can be challenging to achieve with WiFi signals. For UWB technique, the work of [12] proposes a detailed analysis of gait training with depth camera. However, the detected space is also limited to a $3m$ size chamber, which is challenging to demonstrate the applicability of this system to general scenarios. [19] presents a gait recognition system based on RFID technology, utilizing 8 RFID antennas and 6 tags for short-range human gait detection within distances ranging from 0.9m to 2.2m. While their RFID sensing system has demonstrated effectiveness in various scenarios, its deployment method incurs higher costs compared to our LoGait system, which utilizes a single transmitter and two receiver antennas to cover a range of $20m$ in long-distance environments. Meanwhile, the bandwidth of our LoRa methods only take up $125kHz$, which is significantly lower the UWB of $500MHz$ in minimum and WiFi of $300MHz$ in common 802.11n protocol that CSI-tool [20] adopted. Conserving bandwidth resources allows for reliable connectivity and a better network experience for large-scale deployments of IoT applications.

B. Contributions

The problem of recognising humans from their walking patterns is known as gait recognition. It has many potential applications in surveillance, healthcare, and human-computer interaction. In the literature, WiFi-based sensing has provided various solutions for gait recognition [21], [22]. However, the nature of the WiFi signal restricts the sensing range [16], [23]. Therefore, WiFi-based systems cannot be adopted in long-range spaces, e.g., corridors. Inspired by the previous LoRa-based sensing work [24]–[27], we attempt to analyse the feasibility of adopting LoRa sensing in long and narrow environments. We propose LoGait system to push the range of gait recognition to multiple indoor scenarios including a corridor of $20m$ length. The proposed LoGait system is shown in Fig. 1. In summary, the following are the major contributions of this paper.

1) To the best of our knowledge, this study is the first attempt toward using LoRa signals for gait recognition in a 20 meters range.
2) We propose a pipeline for performing preprocessing of LoRa signals for gait feature extraction and classification.
3) We collect LoRa signals containing the gait patterns of different subjects in various scenarios. Our experimental results in different settings validate the effectiveness of our proposed LoGait system in performing gait recognition. Our work fills an absence in this field.

The rest parts of the paper are structured as follows: Section II introduces the preliminary analysis of the LoRa signal. Then it describes the detailed methods for LoRa gait feature extraction, and dynamic time warping (DTW)-based classification.

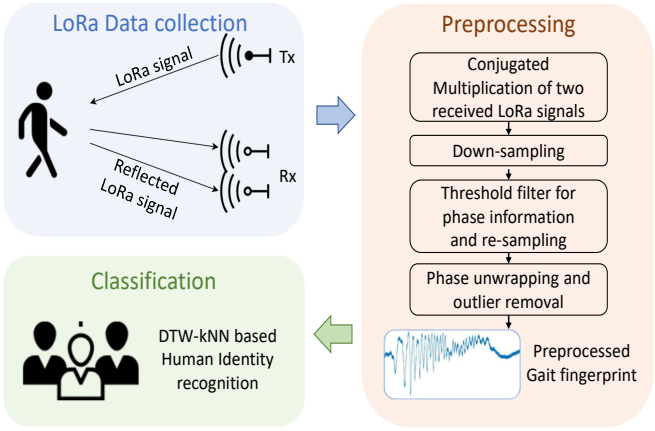

Fig. 1: Overview of proposed LoGait system that consists of three components: (1) LoRa Data Collection; (2) Preprocessing; and (3) Classification using DTW and kNN.

Section III presents the evaluation of the proposed LoGait system in different scenarios.

II. Methodology

A. Preliminaries

Unlike WiFi which applies OFDM to divide channel bandwidth into different subcarriers, LoRa adopts full bandwidth for Chirp Spread Spectrum technology, which encodes information on radio waves using chirp pulses. The technology operates in a fixed-bandwidth channel of 125 kHz for uplink. The frequency of linear chirps increases from $f_c - \frac{B}{2}$ to $f_c + \frac{B}{2}$ over the the sampling period of $-\frac{T_s}{2} < t \leq \frac{T_s}{2}$, where the f_c and T_s represent carrier frequency and sampling time, respectively. The exponential representation of LoRa transmitting signal is composed of two elements, chirp signal and carrier frequency modulation:

$$Tx(t) = e^{j\pi f_s(t) + j2\pi f_c t}, \text{ with } f_s(t) = \pm\frac{B}{T_s}t \tag{1}$$

where, $f_s(t)$ represents the chirp signal with sweep rate. Existing literature on LoRa-based sensing suggests that the channel response at the receiver end can be represented without considering the chirp signal [16]:

$$H(t) = \frac{Rx(t)}{Tx(t)} = e^{-j2\pi\Delta t}(H_s + H_a(t)) + N(t) \tag{2}$$

where, $e^{-j2\pi\Delta f t}$ is due to the sampling frequency offset (SFO) and carrier frequency offset (CFO); $H_s$and $H_a(t)$ represents the LoRa signals from the time-invariant static paths (including the signals in line of sight (LOS) path and those reflected off the stationary objects) and time-variant dynamic paths (including signals reflected from the dynamic objects). $N(t)$ represents the free space transmission noise. LoRa signals in active paths can be expressed as:

$$H_a(t) = \sum_{i=1}^{N_d} a_i(t) e^{-j2\pi\frac{d_i(t)}{\lambda}} \tag{3}$$

where, N_d is the index of path that signal passes through, $a_i(t)$ represents the complex attenuation factor of the i^{th} path; $e^{-j2\pi\frac{d_i(t)}{\lambda}}$ represents the phase change of i^{th} path, with the changing distance of $d_i(t)$ in i^{th} path. λ represents the wavelength of the LoRa signal.

However, the channel response cannot be calculated directly with reference data. In this case, we replicate the setup from previous work with two receiver antennas to get the conjugate multiplication (CM) signal [16], [28]. There are various parameters that correlate with signal ratio. However, to find the dominant dynamic path for estimation, we select two directional antennas which perform better in the reduction of the multipath effect ($N_d = 1$). So we assume in the ideal situation, that there is a single path with relatively less noise ($d_i(t) = d(t)$).

$$\begin{aligned}
R_{CM}(t) &= Rx_1(t)\overline{Rx_2(t)} = Tx(t)\overline{Tx(t)}H_1(t)\overline{H_2(t)} \\
&= Tx(t)\overline{Tx(t)}(e^{-j2\pi\Delta t}(H_{s1} + H_{a1}(t))) \\
&\quad (e^{j2\pi\Delta t}(\overline{H_{s2}} + \overline{H_{a2}(t)})) \\
&= \|Tx\|^2 (H_{s1} + H_{a1}(t))(\overline{H_{s2}} + \overline{H_{a2}(t)}) \\
&= \overbrace{\|Tx\|^2}^{(1)}(\overbrace{H_{s1}\overline{H_{s2}}}^{(2)} + \overbrace{H_{s1}\overline{H_{a2}(t)}}^{(3)} + \overbrace{\overline{H_{s2}}H_{a1}(t)}^{(4)} \\
&\quad + \overbrace{H_{a1}(t)\overline{H_{a2}(t)}}^{(5)})
\end{aligned} \tag{4}$$

From the representation, the components of chirp signal, CFO and SFO are removed. On the other hand, the equation are divided into five parts for analysis: the transmission part of (1) and product of static components of (2) can be regarded as constant value, and the product of active components of (5) is small that can be ignored. Meanwhile, we consider the extended changing path, ΔS, which is caused from the different physical locations of two receiver antennas. Meanwhile, for a short time duration the path anttenuation factor can be regarded as static value. This value is assumed as the constant value due to the setup receiver antennas are close to each other. Next we can rewrite the superposition of rest components in Eq. 5.

$$\begin{aligned}
(3) + (4) &= H_{s1}\overline{H_{a2}(t)} + \overline{H_{s2}}H_{a1}(t) \\
&= H_{s1}(a_2 e^{j2\pi\frac{d(t)+\Delta S}{\lambda}}) + \overline{H_{s2}}(a_1 e^{-j2\pi\frac{d(t)}{\lambda}}) \\
&= (H_{s1}a_2 e^{j2\pi\frac{\Delta S}{\lambda}})e^{j2\pi\frac{d(t)}{\lambda}} + \overline{H_{s2}}a_1 e^{-j2\pi\frac{d(t)}{\lambda}}
\end{aligned} \tag{5}$$

The exponential form can be converted to trigonometric form using Euler's formula and then they can be added together. To summary all, the approximate CM result can be represented as Eq. 6. Meanwhile we replace the representation of $A =$

$H_{s1}a_2e^{j2\pi\frac{\Delta S}{\lambda}}$, and $B = \overline{H_{s2}}a_1$.

$$\begin{aligned} R_{CM}(t) &\approx \|Tx\|^2 (Ae^{j2\pi\frac{d(t)}{\lambda}} + Be^{-j2\pi\frac{d(t)}{\lambda}}) \\ &\approx \|Tx\|^2 (A+B)cos(2\pi\frac{d(t)}{\lambda}) \\ &+ j\|Tx\|^2 (A-B)sin(2\pi\frac{d(t)}{\lambda}) \end{aligned} \tag{6}$$

In this case, we can conclude that both amplitude the phase variation of CM result can be influenced by components from the dynamic path of $d(t)$. which is available to be adopted for gait feature extraction. Experimental validation in Section II-D proves the above conclusion.

B. Preprocessing stages

The inference provided in Section II-A shows that human motion can be indicated by the phase variance of CM results. However, to extract any relevant data related to the motion, it is necessary to go through a series of preprocessing steps before using the Dynamic Time Warping (DTW) recognition. This section outlines all of the steps that we proposed which need to be taken prior to the DTW recognition. All experiment implementation is detailed introduced in Section III.A.(1).

a) Conjugated multiplication of two antennas signal: The Fig. 2 shows the different amplitude of raw LoRa signals with/without dynamic physical interference. Although the envelope shape of LoRa amplitude is explicit, it is required to transform these perturbations into measurable values. Compared to visible variation from amplitude information, phase information shown in Fig. 3c provides random information that cannot be intuitively observed.

In the next step, we observed a considerable number of blank interpolations inside the recieved envelope, which represents the receiver end collected noise during packet duration. Removal of this blank information is important to extract accurate gait features. Firstly, we calculated the CM result from raw LoRa signals of dual antennas, which is shown in Equation. 4. Demonstrated by the Equation, the gain of $\|Tx\|^2$ can determinately increase the amplitude of the received signal, which differentiates the meaningful LoRa signal from noise. From this point of view, the noise duration can be removed by setting the low amplitude threshold of CM result. In Fig. 3a, the red dashed line represents signal components from noise and the green one from the LoRa chirp signal. Meanwhile, we assume the transmitted power of LoRa signals and free space attenuation is stable. In this case, the threshold was set to the mean value of the first second's receiving signals.

b) Threshold filter for phase information and downsampling: Meanwhile, there are two downsample operations executed before and after threshold filtering. For amplitude threshold, it is a waste of computational resources for searching and comparing all $800k$ samples per second. On the other hand, the Doppler shift frequency range that human activity can generate is limited to $60Hz$ [29], $800kHz$ sampling rate is highly redundant. Therefore, we set the first downsample of $1k$ sample rate ahead of threshold operation. In practical scenario, there must be a silent duration while transmitting chirp signals to reduce the power consumption and avoid interference among different packages by multipath effect, which is called Inter-Symbol Spacing (ISS). However, the receiver side is not able to differentiate if received samples belongs to ISS. In this case, we adopt an adaptive thresholding calculation method to filter the ISS information out of gait profile. At first we statically sorted the non-zero value of CM results and pick the smaller components of whole CM sequence based on the percentage that ISS occupies. The priority assumption is that under silent conditions, the receiver can only get a noisy signal with a stable amplitude and a spurious phase, which are shown in Fig. 3a and Fig. 3b. By calculating the mean and standardized variation of estimated ISS information, we can determine the value of threshold. To make it more generalised, the value is set to the mean plus double standardised value. After performing thresholds filtering, we discovered that the length of the LoRa chirp signal is not constant. Then, we resample the filtered data to $1kHz$ for unifying constant sampling frequency among different profiles. Fig. 3c shows the LoRa signal after threshold filtering with twice downsampling.

c) Phase unwrapping and outlier removal: In this stage, we acquire meaningful phase information that can reflect the channel environment. However, the outliers and mismatched phase data appear. We adopt the Hampel filter and unwrap operation to denoise the signals, with the shown comparison figures shown in Fig. 4. The signal components that are framed out by a red box represent the recovered parts by the methods.

C. Gait analysis

Considering the ISS, we only adopt the phase of CM sequence for gait analysis. According to the Eq. 6, the phase is given as follows:

$$\Delta\phi_{R_{CM}} = \|Tx\|^2 (A-B)sin(2\pi\frac{d(\Delta t)}{\lambda}) \tag{7}$$

where $\|Tx\|^2 (A-B)$ can be treated as constant. Then we take the derivative of this equation, the period of the phase change is related to the dynamic path $d(t)$. In this case, the system can be considered as a monocular radar system, which represents the path length of moving target should be considered twice of varying distance: $d(\Delta t) \approx 2\Delta d$. In this case we can get the $\Delta\phi_{R_{CM}} \propto sin(4\pi\frac{\Delta d}{\lambda})$. By leveraging the periodic nature of the sinusoidal signal, we can deduce the distance the monitored object has traversed by inverting the observed phase period. We name the periodicity of $\phi_{R_{CM}}$ as T, and get $T = 2\frac{\Delta d}{\lambda}$. Meanwhile, the wavelength of LoRa signal is fixed to $\lambda = c/f = \frac{3\times10^8}{868.1\times10^6} = 0.346m$. From the equation we can get the moving distance of target is related to the periodicity of phase variation, which is $\Delta d = 0.173T$. Then, to verify the above derived equation formula, we collected moving data from a humanoid robot and a human volunteer moving $2m$ in fixed area respectively, shown in Fig. 5. All the peaks are labeled with dotted line. In the robot moving profile, we observed 11 peaks and 10 periods of signals, which represents the minimum of moving distance of robot reaches

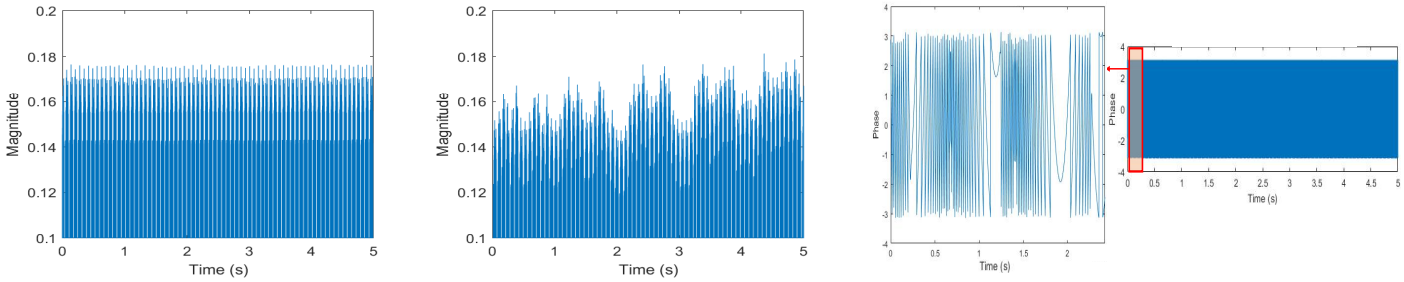

(a) Amplitude of static scenario (b) Amplitude of single person walking in LOS range (c) Raw phase signal of LoRa signal

Fig. 2: Amplitude and phase plots of raw LoRa signals.

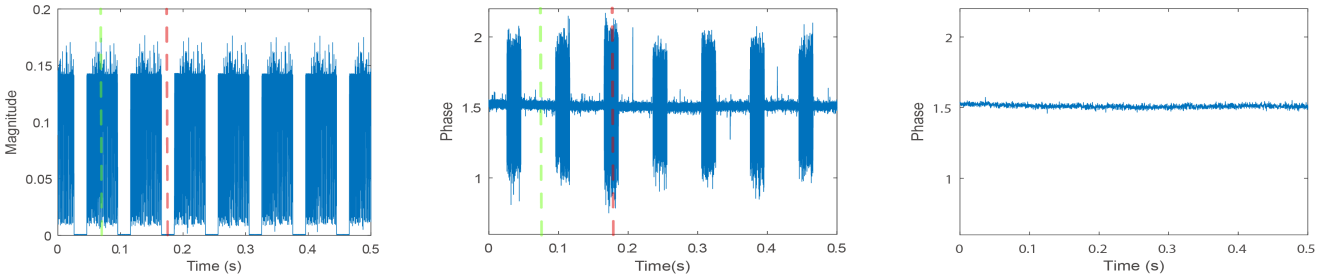

(a) Amplitude plot (b) Phase plot (c) Phase plot after threshold filter

Fig. 3: Plot of CM results under static environment with the red dashed line labelled for noise components and green one for LoRa chirp signals in (a) and (b).

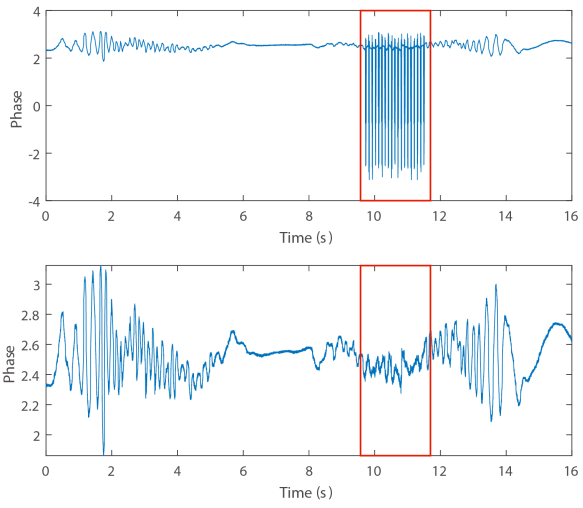

Fig. 4: Comparison plots with/without Hampel filter and phase unwrapping, with circled outliers in red boxes. The first graph shows original gait signals and the second shows Hampel filtered and phase-unwrapped gait signals.

$1.73m$. Considering the start and end period are not properly counted, the result is close to $2m$. However, instead of robot profile, the human profile illustrates 14 peaks, which represents the distinct motion beyond $2m$. Meanwhile, we discover that there are some fluctuated peaks having less amplitude variation than torso motion, which is labeled in red block. Excluding the possibility of environmental influences, this part of the correspondence could only be generated by the movement of the limbs. Therefore, in the robot scenario, the phase change only reflects by $2m$ displacement. In the human scenario, the phase change is caused mainly by both displacement of body torso motion and waving limbs.

Although the processed signal contains all gait information of subject, these information is difficult to quantified and modeled accurately due to the complex dynamical structure of realistic human gait. However, there is a prerequisite that different human's gait schemes are different [30]. By constructing a database of LoRa signals generated by the gait of different volunteers, we can use statistical-based machine learning methods to find differences in the gait of identity.

D. DTW-based Gait Recognition

After preprocessing of LoRa signals, we compared the signals collected from different activities and gait signals, shown in Fig. 6. The gait experiment setup is the same as LOS experiment that mentions in Section. III-A.

From the intuitive view, we observed the collected activity signals under three different scenarios that match our normal experiences: the human presence scene only contains chest motion of respiration, and stepping signals contains multiple signal peaks from human skeleton motion. From the gait

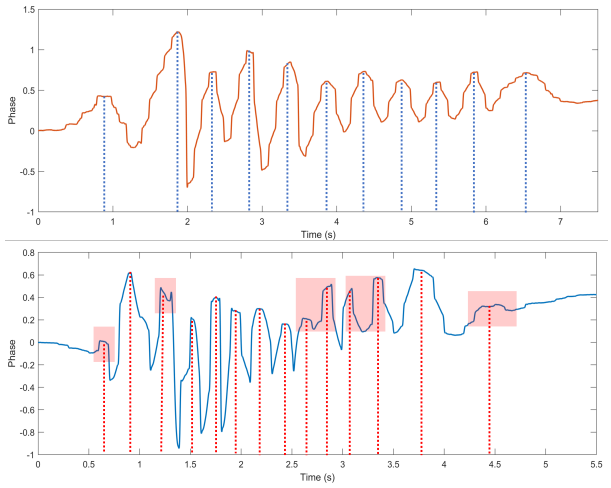

Fig. 5: Gait profiles of humanoid robot motion (first graph) and human volunteer (second graph).

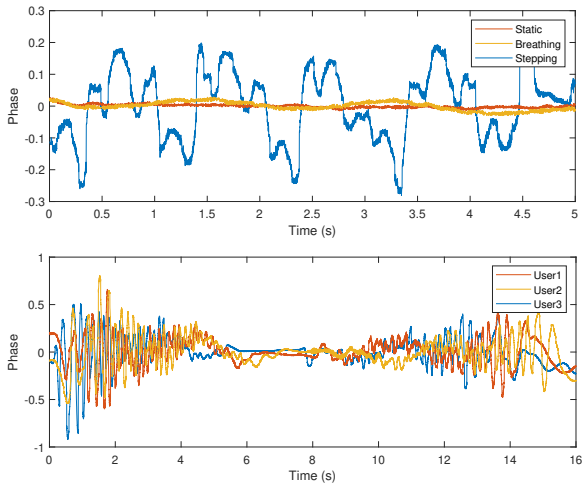

Fig. 6: Comparison of LoRa signals under different scenarios of no-person, a person standing still, a person stepping shown in the first figure; and gait profiles of three users in the second figure.

profiles of three users, we found that the human behaviour patterns of different identities are highly overlapping compared to human activity recognition. Besides, there are two main challenges that were observed in the comparison:

1) Variation of motion speed can result in various lengths of gait signals from a single subject.
2) Temporal gait signal can not be completely aligned while the data collection, which causes the distortion of information.

The general method of measuring the similarity of two-time series signals is to calculate the Euclidean distance. However, lock-step Euclidean distance measurement refers to those distances that compare the ith point of one series to the ith point of another, which is significantly influenced by incomplete alignment [31]. To solve the alignment problem and improve the recognition performance, DTW based method was adopted.

DTW is a similarity measurement method, which exhausts all the correspondences with restrictions and finds the one with the smallest distance. Then the cumulative distance of the selected path is used for their similarity judgement. The Equation. 8 describes the algorithm of DTW distance.

$$D_{min}(i,j) = M(i,j) + min \begin{cases} D(i-1,j-1) \\ D(i-1,j) \\ D(i,j-1) \end{cases} \quad i,j \geq 1 \tag{8}$$

To align the two sequences, a matrix with two dimensions of sequences' length is required. The matrix element $M(i,j)$ denote the Euclidean distance $d(x_i, y_j)$ between the two points x_i and y_j. The shortest distance of the current element $D_{min}(i,j)$ is necessarily the length of the shortest path of the previous element plus the value of the current element. There are three possible directions for the previous element, so we take the minimum value of three possibilities into DTW distance.

For initial validation of DTW, we calculated the DTW distance of gait profiles of different identities and the same identity respectively to verify the algorithm's availability. The comparison graph is shown in Fig. 7 which illustrated the distance between the same user and different users. The larger DTW distance verified our assumption that the gait profiles of different identities have mismatched information and the data from a single identity has similar features. Therefore, we adopted a K-nearest neighbour (KNN) cluster-based algorithm to classify different identities of gait signals.

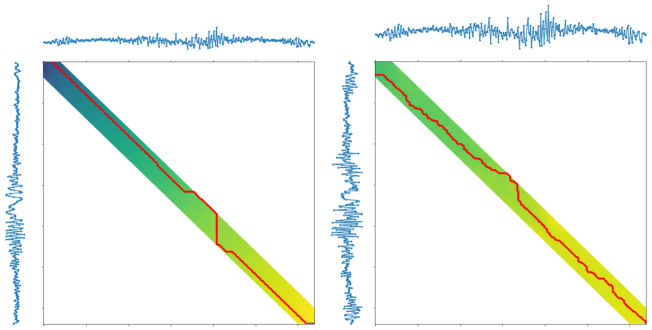

(a) DTW distance: 5.81 (b) DTW distance: 0.36

Fig. 7: Comparison of DTW distance matrix of (a) gait profiles from the first user and second user; (b) gait profiles from the first user.

III. Evaluation

A. Experiment Setup

1) Devices: Our implementation considers one pair of devices to imitate the general LoRa link. We select one USRP b205mini and one USRP x310 as transmitter and receiver, respectively. On the transmitting side, we have opted for a directional linear polarized antenna of Aaronia Ag. This type

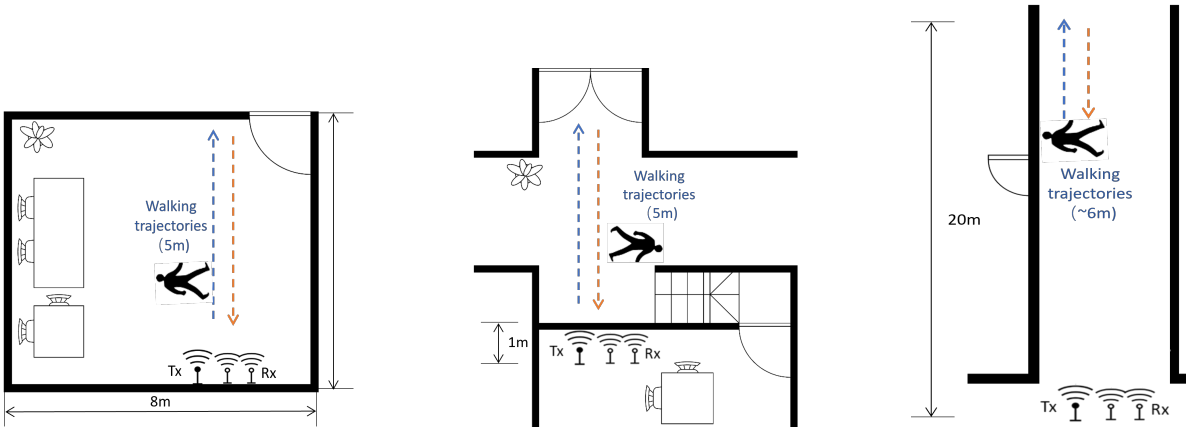

(a) Line of Sight (LOS) (b) Non Line of Sight (NLOS) (c) Long Distance (LD)

Fig. 8: Experimental setup of 3 scenarios.

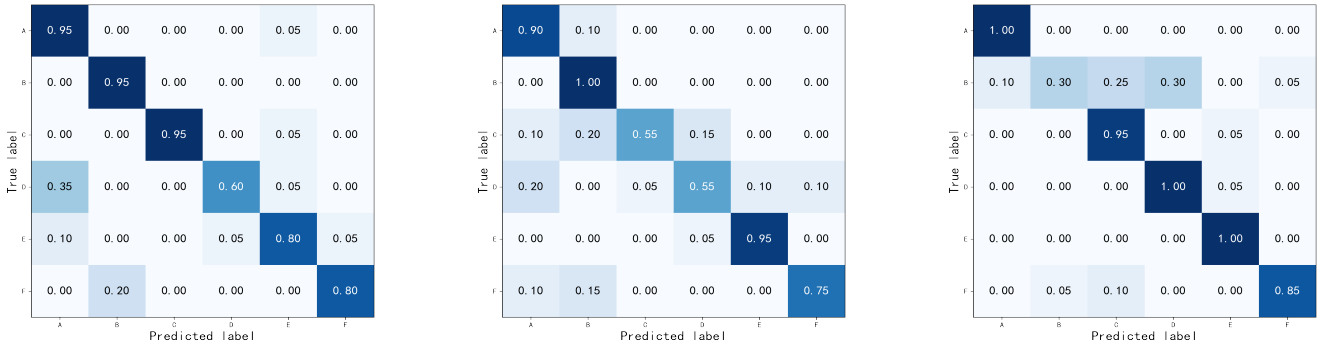

(a) LOS (b) NLOS (c) LD

Fig. 9: Confusion matrix of gait recognition in 3 scenarios

of antenna emits signals in a specific direction, allowing us to focus the transmission towards the target area, namely the long corridor under observation. The directional nature of this antenna ensures that the transmitted signals are concentrated along a desired path, enhancing the accuracy of gait information collection. On the receiving side, we have implemented two antennas of SlimLine A5010 Circular Polarized Antenna with 8.5 dBi gain. Circular polarized antennas are known for their ability to capture signals from various polarization angles, making them suitable for scenarios where the incoming signals may have different polarization orientations. By utilizing a circular polarized antenna, we can effectively receive the transmitted signals, regardless of their polarization alignment. Moreover, our choice of directional and circular polarized antennas offers an advantage in mitigating the impact of multipath propagation. With an omni-directional antenna, signals can bounce off obstacles and create interference due to multipath reflections. However, by utilizing directional antennas, we can minimize the reception of reflected signals and primarily capture signals from the intended pointing direction. This helps to reduce the effects of multipath interference, improving the reliability and accuracy of the gait information obtained. The LoRa signal is generated by an open-source project of LoRa communication in the physical layer [32]. On the receiver side, we configured Labview based system to collect LoRa signal. The experimental setup can be viewed in Fig. 10. The sampling rate and packet duration are set to $800kHz$ and $20ms$, respectively.

2) Application scenarios: The experiments were conducted in 3 different scenarios: line of sight (LOS), non-line of sight (NLOS) and long distance (LD) range, with the top-view structure graph shown in Fig. 8. In the LOS scenario, the room area occupied for the activity experiment is $6m$ in length and $5m$ in width. One line has marked a $5m$ distance on which people walk to and from the front of the transmitter and receiver. In NLOS scenario, all apparatus containing the transmitter and receiver are in one room, and activity is being monitored outside of the room, shown as walking trajectories. The space between devices and humans is separated by a brick wall. In the LD scenario, the implementation is setup in

a corridor of $20m$ length. Volunteers were arranged to walk along the trajectory at the end of the corridor, shown in Fig. 10.

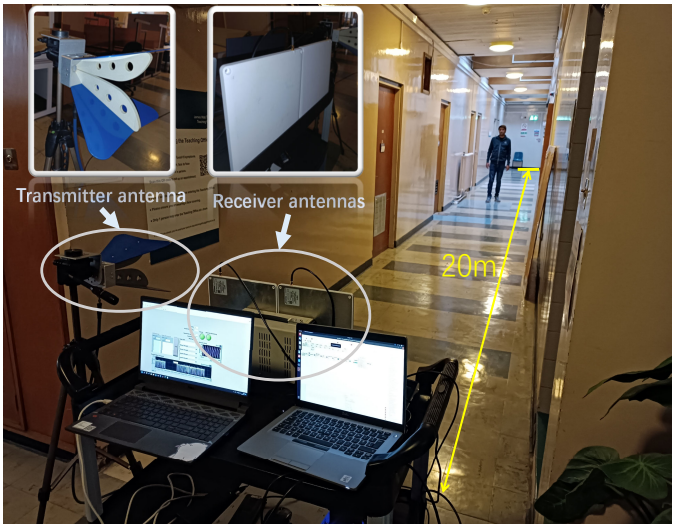

Fig. 10: Experimental setup in Long distance scenario

3) Gait profiles: The basic human gait in our experiment contains three phases: rotating, walking and standing. In this study, our focus was primarily on the identification of gait patterns in single-person walking scenarios. Meanwhile we discuss the challenges posed by multiple walking scenarios in Section III-B6 of the paper. During one data collection, one person was asked to turn back, and walk along the trajectory and stand still for 8 seconds. Then, it took another 8 seconds for subjects to walk back to the starting point. The gait signal in each profile lasts for 16 seconds in total. Besides, we downsample the signals to $200Hz$ for speeding up the machine learning algorithm.

We recruited 13 volunteers for data collection of human gait including 4 females and 9 males. This human involved research has got the ethic approval from College of science and engineering from University of Glasgow, approval no: 300210309. In each scenario, we ask 6 subjects to conduct the experiments and data was collected for 20 rounds for each person that provides $16s$ gait data. In total, we have collected 5744 seconds of gait signals for experimental validation.

B. Overall performance and Discussion

The recognition performance of 3 scenarios with confusion matrices is shown in Fig. 9. We perform a 5-fold cross-validation on collected data with an overall accuracy of 85.13% in LOS range, 79.13% in NLOS and 84.14% in LD respectively. The average accuracy of 82.8% validates the effectiveness of our system. To study the performance of the LoGait system affected by different factors, we design the comparison tests and analyse the influence of Sample rate, Classification distance algorithm. Meanwhile, we explain the difference in Data collection methods of gait signal between LOS/NLOS and LD scenarios.

1) Sample Rate: The sample rate of gait profiles is the significant parameter that balance of recognition performance and processing speed. We resample the gait profiles from $10Hz$ sample rate to $500Hz$ to test the performance of the LoGait system. The recognition performance is illustrated in Fig. 11, which validates that a higher sample rate preserves more gait information.

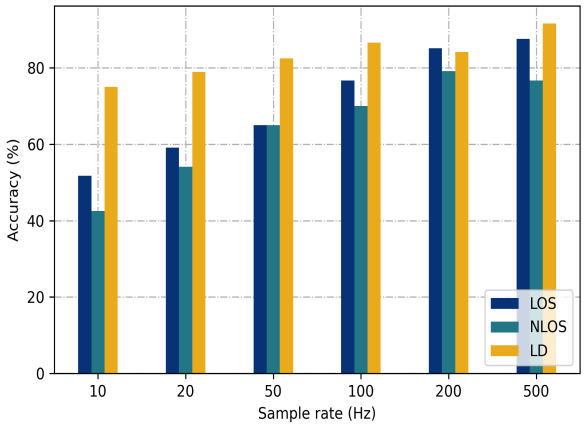

Fig. 11: Recognition accuracy via sample rate in 3 scenarios

2) Vector distance algorithm: To approve the assumption in Section. II-D, we compared the classification results using the other three distance algorithms with DTW distance, shown in Fig. 12. It illustrated that the DTW-based classification method acquires the best performance among the traditional distance estimation algorithms.

3) Walking directions: In our experiment, we divided the data collection of one profile into two phases, moving forward and back, as shown in Fig. 8 (depicted by blue and red dashes). To effectively evaluate the performance of our system, we separated the profile into three parts: forward, back, and integration.

4) Data collection methods: In both LOS and NLOS scenarios, we asked volunteers to do free walking in a restricted space. In this case, the users are easy to control their speed without following usual habits. To study the robustness of the gait recognising system, in the LD scenario, the volunteers were asked to walk freely in a given time slot instead of limiting the moving area. From the results, the accuracy under the LD environment approves the popularization potential of the LoGait system.

5) Strength influence: In this section we complement the LoGait identification performance on different signal strength condition by analysing human and moving robot gait profiles under the same environment. From the Eq. 6, we know the CM result is significantly influenced by transmission gain of communication system. In the absence of environmental changes, the noise in the received signal will remain stable, but resulting in varying gain of human related moving signals due to changes in transmission gain. Intuitively, we assume that lower signal strength will diminish the stylized components of the gait, leading to increasingly noise which damages

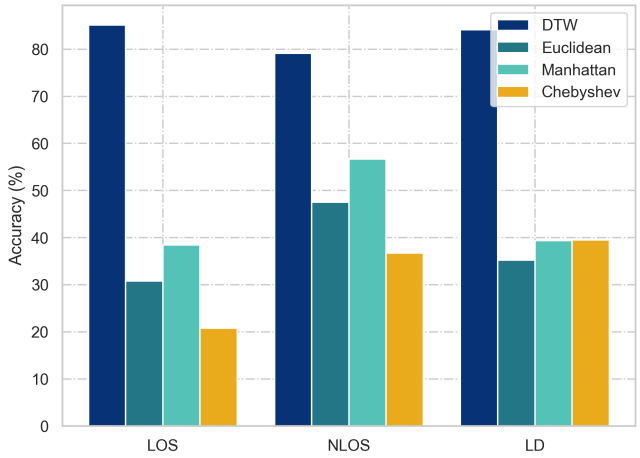

Fig. 12: Recognition accuracy of distance algorithms in 3 scenarios

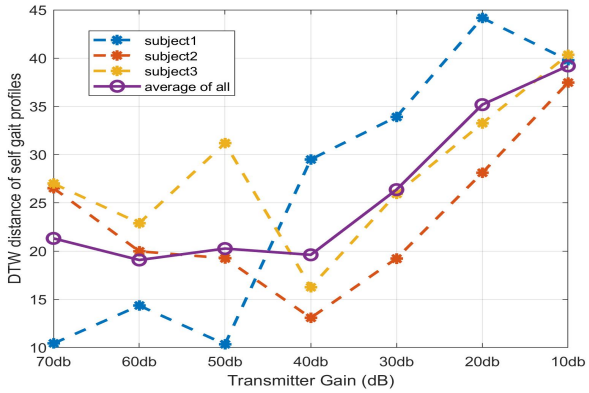

Fig. 13: DTW distance between two profiles from single subject via Transmitter Gain

the similarity between gait signals. In this case, we set the fixed trajectory of single person, and recollect LoRa signals in different transmitter gain. By manipulating the transmitted signal strength, we compute the euclidean distance after DTW operation between the two motion profiles of human subject himself/herself. As we decrease the signal strength, we expect to observe a increase of the DTW distance, indicating the noise interferes with the gait signals between gait patterns from same person. Larger DTW distance represents the system prefers to split two profiles of the same category into two different parts, which can be predicted to reduce the accuracy of the system for identification. The result of mentioned experiments from three volunteers is shown in Fig. 13. At gains higher than $40dB$, we observed random variations in the DTW distance of the three subjects, which can be attributed to the natural variation in their respective gaits. However, beyond the $40dB$ gain threshold, all three trends exhibited an upward trend, indicating that the noise components were increasingly dominating the gait profiles and diminishing the relevance of individual gait patterns. This outcome aligns with our assumption that lower signal strength significantly hampers the identification recognition capabilities of our system.

Consequently, distinguishing between different individuals becomes more challenging under the scenario of lower transmission gain for the models employed in this study.

6) Multiple scenarios: Recently, we only utilise single transmitter and phase difference of a pair of LoRa channels. The prerequisite for identification in a multi-person environment is to obtain the complete gait signal of each person. Typically, both the extraction of beamforming signals in a specific azimuth direction and independent component analysis have the potential to perform blind source separation of gait signals. However, due to the limitations of the experimental apparatus, the only signals we obtained were a set of phase differences computed from the two channels. Therefore, the received signals can not provide independent signals for multiple gait

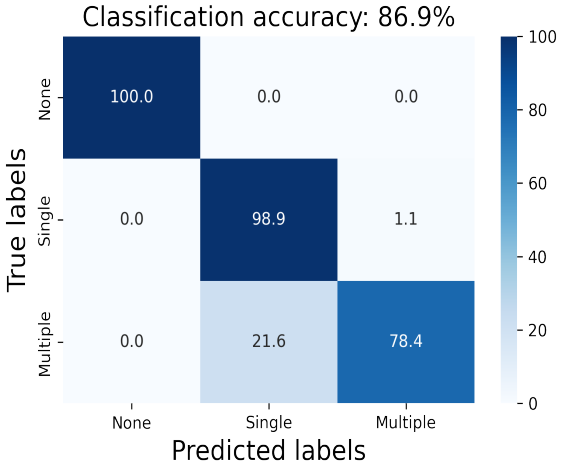

Fig. 14: Recognition accuracy of LD scenario with different amount of walking subjects

identification recognition. Separating and analysing distinct gait signals will be our next stage target.

Although the recent LoGait system is not able to complete identification recognition in multiple targets scenario, it has the ability to distinguish the number of targets walking in sensing area. We collected data from five different classes, involving the empty environment and individuals walking. The number of participants ranged from 1 to 4. Considering the size of walking area, we selected LD scenario for experiments. And collect 10 minutes for all participants' random walking which is the same as the single LD experiment setup. To implement as the realtime setup, we totally collect 472 profiles for by extracting the profile of 50 minutes data. By using proposed classification scheme, the average accuracy that detect scenarios arrives at 86.9%, shown in Fig. 14. The result proves that the system has limited ability to capture response from multiple human walking pattern. In the next step, we will work on solving the multiple gait separation and recognition with multiple-channel device.

IV. Conclusion

This paper presents the LoGait system, a novel approach for human gait recognition in various indoor scenarios, including living rooms, through-wall scenarios, and corridors. The system analyzes the feasibility of LoRa sensing and employs conjugated multiplication, along with multiple preprocessing methods, to extract LoRa gait profiles. These methods focus on filtering communication symbols and extracting physical variation information from human gait. User identity recognition is achieved using a DTW-based machine learning algorithm. Experimental evaluations in three scenarios demonstrate promising results, with an identification accuracy of 85.13% in living rooms, 79.13% in through-wall scenarios, and 84.14% in $20m$ corridors. By addressing complex indoor environments, including through-wall scenarios and long-distance corridors, the LoGait system represents a significant advancement in gait recognition prototypes with great potential.

Acknowledgements

This work was supported in parts by Engineering and Physical Sciences Research Council (EPSRC) grants EP/T021020/1, EP/T021063/1 and EP/W003228/1.

References

[1] H. Hameed, M. Usman, A. Tahir, A. Hussain, H. Abbas, T. J. Cui, M. A. Imran, and Q. H. Abbasi, "Pushing the limits of remote rf sensing by reading lips under the face mask," *Nature Communications*, vol. 13, pp. 5168–5176.

[2] M. Usman, J. Rains, T. J. Cui, M. Z. Khan, M. A. Imran, Q. H. Abbasi *et al.*, "Intelligent wireless walls for contactless in-home monitoring," *Light: Science & Applications*, vol. 11, pp. 212–224, 2022.

[3] W. Li, B. Tan, and R. Piechocki, "Passive radar for opportunistic monitoring in e-health applications," *IEEE journal of translational engineering in health and medicine*, vol. 6, pp. 1–10, 2018.

[4] Y. Ge, A. Taha, S. Shah, K. Dashtipour, S. Zhu, J. M. Cooper, Q. Abbasi, and M. Imran, "Contactless wifi sensing and monitoring for future healthcare - emerging trends, challenges and opportunities," *IEEE Reviews in Biomedical Engineering*, pp. 1–1, 2022.

[5] Y. Ma, G. Zhou, and S. Wang, "Wifi sensing with channel state information: A survey," *ACM Computing Surveys (CSUR)*, vol. 52, no. 3, pp. 1–36, 2019.

[6] L. Lee and W. E. L. Grimson, "Gait analysis for recognition and classification," in *Proceedings of Fifth IEEE International Conference on Automatic Face Gesture Recognition*. IEEE, 2002, pp. 155–162.

[7] C. Wan, L. Wang, and V. V. Phoha, "A survey on gait recognition," *ACM Computing Surveys (CSUR)*, vol. 51, no. 5, pp. 1–35, 2018.

[8] W. Wang, A. X. Liu, M. Shahzad, K. Ling, and S. Lu, "Device-free human activity recognition using commercial wifi devices," *IEEE Journal on Selected Areas in Communications*, vol. 35, no. 5, pp. 1118–1131, 2017.

[9] J. Ding and Y. Wang, "Wifi csi-based human activity recognition using deep recurrent neural network," *IEEE Access*, vol. 7, pp. 174 257–174 269, 2019.

[10] L. Zhang, C. Wang, M. Ma, and D. Zhang, "Widigr: Direction-independent gait recognition system using commercial wi-fi devices," *IEEE Internet of Things Journal*, vol. 7, no. 2, pp. 1178–1191, 2020.

[11] D. Wang, J. Yang, W. Cui, L. Xie, and S. Sun, "Caution: A robust wifi-based human authentication system via few-shot open-set recognition," *IEEE Internet of Things Journal*, vol. 9, no. 18, pp. 17 323–17 333, 2022.

[12] S. P. Rana, M. Dey, M. Ghavami, and S. Dudley, "Markerless gait classification employing 3d ir-uwb physiological motion sensing," *IEEE Sensors Journal*, vol. 22, no. 7, pp. 6931–6941, 2022.

[13] H. Li, J. Le Kernec, A. Mehul, S. Z. Gurbuz, and F. Fioranelli, "Distributed radar information fusion for gait recognition and fall detection," in *2020 IEEE Radar Conference (RadarConf20)*. IEEE, 2020, pp. 1–6.

[14] C. Ding, L. Zhang, C. Gu, L. Bai, Z. Liao, H. Hong, Y. Li, and X. Zhu, "Non-contact human motion recognition based on uwb radar," *IEEE Journal on Emerging and Selected Topics in Circuits and Systems*, vol. 8, no. 2, pp. 306–315, 2018.

[15] A. Jayatilaka and D. C. Ranasinghe, "Real-time fluid intake gesture recognition based on batteryless uhf rfid technology," *Pervasive and Mobile Computing*, vol. 34, pp. 146–156, 2017.

[16] F. Zhang, Z. Chang, K. Niu, J. Xiong, B. Jin, Q. Lv, and D. Zhang, "Exploring lora for long-range through-wall sensing," *Proceedings of the ACM on Interactive, Mobile, Wearable and Ubiquitous Technologies*, vol. 4, no. 2, pp. 1–27, 2020.

[17] Z. Zhang, Z. Tian, and M. Zhou, "Latern: Dynamic continuous hand gesture recognition using fmcw radar sensor," *IEEE Sensors Journal*, vol. 18, no. 8, pp. 3278–3289, 2018.

[18] F. Zhang, Z. Chang, K. Niu, J. Xiong, B. Jin, Q. Lv, and D. Zhang, "Exploring lora for long-range through-wall sensing," *Proc. ACM Interact. Mob. Wearable Ubiquitous Technol.*, vol. 4, no. 2, jun 2020. [Online]. Available: https://doi.org/10.1145/3397326

[19] Y. Chen, J. Yu, L. Kong, Y. Zhu, and F. Tang, "Rfpass: Towards environment-independent gait-based user authentication leveraging rfid," in *2022 19th Annual IEEE International Conference on Sensing, Communication, and Networking (SECON)*, 2022, pp. 289–297.

[20] D. Halperin, W. Hu, A. Sheth, and D. Wetherall, "Tool release: Gathering 802.11n traces with channel state information," *SIGCOMM Comput. Commun. Rev.*, vol. 41, no. 1, p. 53, jan 2011. [Online]. Available: https://doi.org/10.1145/1925861.1925870

[21] W. Wang, A. X. Liu, and M. Shahzad, "Gait recognition using wifi signals," in *Proceedings of the 2016 ACM International Joint Conference on Pervasive and Ubiquitous Computing*, 2016, pp. 363–373.

[22] Y. Zhang, Y. Zheng, G. Zhang, K. Qian, C. Qian, and Z. Yang, "Gaitid: robust wi-fi based gait recognition," in *International Conference on Wireless Algorithms, Systems, and Applications*. Springer, 2020, pp. 730–742.

[23] Y. Zeng, D. Wu, J. Xiong, E. Yi, R. Gao, and D. Zhang, "Farsense: Pushing the range limit of wifi-based respiration sensing with csi ratio of two antennas," *Proc. ACM Interact. Mob. Wearable Ubiquitous Technol.*, vol. 3, no. 3, sep 2019. [Online]. Available: https://doi.org/10.1145/3351279

[24] B. Xie, Y. Yin, and J. Xiong, "Pushing the limits of long range wireless sensing with lora," *Proceedings of the ACM on Interactive, Mobile, Wearable and Ubiquitous Technologies*, vol. 5, no. 3, pp. 1–21, 2021.

[25] B. Xie and J. Xiong, "Combating interference for long range lora sensing," in *Proceedings of the 18th Conference on Embedded Networked Sensor Systems*, 2020, pp. 69–81.

[26] F. Zhang, Z. Chang, J. Xiong, and D. Zhang, "Exploring lora for sensing," *GetMobile: Mobile Computing and Communications*, vol. 25, no. 2, pp. 33–37, 2021.

[27] F. Zhang, Z. Chang, J. Xiong, R. Zheng, J. Ma, K. Niu, B. Jin, and D. Zhang, "Unlocking the beamforming potential of lora for long-range multi-target respiration sensing," *Proceedings of the ACM on Interactive, Mobile, Wearable and Ubiquitous Technologies*, vol. 5, no. 2, pp. 1–25, 2021.

[28] Y. Zeng, D. Wu, R. Gao, T. Gu, and D. Zhang, "Fullbreathe: Full human respiration detection exploiting complementarity of csi phase and amplitude of wifi signals," *Proc. ACM Interact. Mob. Wearable Ubiquitous Technol.*, vol. 2, no. 3, sep 2018. [Online]. Available: https://doi.org/10.1145/3264958

[29] K. Qian, C. Wu, Y. Zhang, G. Zhang, Z. Yang, and Y. Liu, "Widar2. 0: Passive human tracking with a single wi-fi link," in *Proceedings of the 16th Annual International Conference on Mobile Systems, Applications, and Services*, 2018, pp. 350–361.

[30] C. Wan, L. Wang, and V. V. Phoha, "A survey on gait recognition," *ACM Comput. Surv.*, vol. 51, no. 5, aug 2018. [Online]. Available: https://doi.org/10.1145/3230633

[31] A. Abanda, U. Mori, and J. A. Lozano, "A review on distance based time series classification," *Data Mining and Knowledge Discovery*, vol. 33, no. 2, pp. 378–412, 2019.

[32] J. Tapparel, O. Afisiadis, P. Mayoraz, A. Balatsoukas-Stimming, and A. Burg, "An open-source lora physical layer prototype on gnu radio," in *2020 IEEE 21st International Workshop on Signal Processing Advances in Wireless Communications (SPAWC)*. IEEE, 2020, pp. 1–5.